Rawal, S., Sinha, R.K., and De La Rue, R. (2012) Silicon-on-insulator photonic crystal miniature devices with slow light enhanced third-order nonlinearities. Journal of Nanophotonics, 6 (1). 063504. ISSN 1934-2608

http://eprints.gla.ac.uk/69345

Deposited on: 07 September 2012

Enlighten – Research publications by members of the University of Glasgow
http://eprints.gla.ac.uk

Journal of Nanophotonics

SPIEDigitalLibrary.org/jnp

Silicon-on-insulator photonic crystal miniature devices with slow light enhanced third-order nonlinearities

Swati Rawal
Ravindra K. Sinha
Richard M. De La Rue

SPIE

Downloaded From: http://nanophotonics.spiedigitallibrary.org/ on 09/07/2012 Terms of Use: http://spiedl.org/terms

Silicon-on-insulator photonic crystal miniature devices with slow light enhanced third-order nonlinearities

Swati Rawal,[a] Ravindra K. Sinha,[a] and Richard M. De La Rue[b,c]
[a]Delhi Technological University (Formerly Delhi College of Engineering),
TIFAC-Centre of Relevance and Excellence in Fiber Optics and Optical Communication,
Department of Applied Physics, Bawana Road, Delhi-110042, India
E-mail: dr_rk_sinha@yahoo.com
[b]University of Malaya, Photonics Research Centre, Physics Department, Science Faculty,
50603 Kuala Lumpur, Malaysia
[c]University of Glasgow, Optoelectronics Research Group, School of Engineering,
Rankine Building, Oakfield Avenue, Glasgow G12 8LT, Scotland, United Kingdom

Abstract. The effects of the slow-down factor on third-order nonlinear effects in silicon-on-insulator photonic crystal channel waveguides were investigated. In the slow light regime, with a group index equal to 99, these nonlinear effects are enhanced but the enhancement produced depends on the input peak power level. Simulations indicate the possibility of soliton-like propagation of 1 ps pulses at an input peak power level of 50 mW inside such a photonic crystal waveguide. The increase in the induced phase shift produced by lower group velocities can be used to decrease the size and power requirements needed to operate devices such as optical switches, logic gates, and wavelength translators. © *2012 Society of Photo-Optical Instrumentation Engineers (SPIE).* [DOI: 10.1117/1.JNP.6.063504]

Keywords: slow light; nonlinear optics; photonic crystals.

Paper 11103 received Sep. 28, 2011; revised manuscript received Nov. 23, 2011; accepted for publication Nov. 30, 2011; published online Mar. 12, 2012.

1 Introduction

Slow light refers to a reduced group velocity and it offers major opportunities for controlled enhancement of light-matter interaction. High-refractive-index-contrast structures such as photonic crystal (PhC) waveguides have been demonstrated to be a promising approach to the achievement of slow light behavior.[1] Linear effects such as gain, the thermo-optic effect, and some types of electro-optic interaction, scale linearly with the slow-down factor, whereas nonlinear effects such as two-photon absorption (TPA) and Kerr nonlinearity, scale with the square of the slow-down factor.[2,3] The spatial compression experienced by light when it goes from a fast light situation to a slow light situation, and the greater time that light spends in the waveguide, because of the slow group velocity, increase the strength of the light-matter interaction, and together imply the enhancement of nonlinear effects. Thus slow light behavior causes a reduction in the input power level and the physical length of the waveguide needed to produce given magnitudes of linear and nonlinear effects, by comparison with propagation in the fast light regime.[2,4]

By carefully engineering the photonic dispersion relationship, one may obtain unique opportunities for the realization of devices that exploit slow light effects.[5] Recently, nonlinear effects such as the Raman effect, soliton propagation, TPA, etc., have been observed by several different groups[6–10] in different types of waveguide structures. Self-phase modulation (SPM), which leads to chirping and spectral broadening of ultra-short pulses, has also been previously reported, in silicon optical waveguides.[8] However, TPA limits the extent of SPM through nonlinear absorption.[11] TPA typically involves transitions from the ground state of a system to a higher state by absorption of two photons from an incident radiation field having identical, or more generally, two different frequencies. TPA further creates free carriers that lead to additional losses through free-carrier absorption (FCA), and refractive index changes through free-carrier dispersion

0091-3286/2012/$25.00 © 2012 SPIE

Downloaded From: http://nanophotonics.spiedigitallibrary.org/ on 09/07/2012 Terms of Use: http://spiedl.org/terms

(FCD).[12–14] Thus, TPA, FCA, FCD, and SPM are important effects that influence the behavior of short laser pulses in silicon waveguides.

Soliton dynamics will dominate the propagation of femtosecond pulses in PhC waveguides when the group velocity dispersion (GVD) is strongly anomalous because of large waveguide dispersion.[9] It is important to mention that, as optical pulses propagate through photonic crystal waveguides; their evolution in both the time and frequency domains is governed by the interplay of linear dispersion and nonlinearity. These effects are characterized by the characteristic lengths: namely the GVD length, LD, and the nonlinear length N_{NL} (Ref. 15). Depending on the relative magnitudes of L_D, N_{NL}, and the waveguide length, L, pulses evolve in various different ways. Here, $L_D = T_0^2/|\beta_2|$, $L_{\mathrm{NL}} = 1/\gamma P_{\mathrm{in}}$, where T_0 is the initial width, in time, of the pulse, P_{in} is the incident power, β_2 is the GVD parameter, and γ is the nonlinear parameter defined in subsequent sections.

Monat and colleagues[16] have described how slow light with a group velocity on the order of $c/50$ can be obtained in silicon based PhC waveguides with an air-bridge or membrane structure. Such structures are inherently mechanically vulnerable. Monat and colleagues[16] have also shown that dispersion engineered slow-light PhC waveguides provide a suitable platform for enhancing nonlinear effects, making it possible to realize compact, low-power, all-optical signal processing devices.

For Gaussian pulses, an important criterion for comparing the relative magnitudes of the effects labelled as FCA, FCD and TPA comes from the dimensionless parameter:[17] $r_a = (S\sigma P_{\mathrm{in}} T_0 \sqrt{\pi})/(2\sqrt{2}\hbar\omega_o A_{\mathrm{eff}})$, where S is the slow-down factor, σ is the FCA coefficient, P_{in} is the peak input power, and A_{eff} is the effective area of cross-section. The free carrier density near the input end of the waveguide is negligible when $r_a \ll 1$, i.e., the pulse peak power level is relatively low (e.g., a value of 100 mW in the context of this paper). In this situation, only TPA comes into play to a significant extent, and the observed reduction in output power is almost solely due to TPA. In this work, we investigated the propagation of light in a nonlinear slow-light medium formed by a channel waveguide in a silicon-on-insulator (SOI) photonic crystal structure with *elliptically* shaped holes in a silicon core, and mechanically supported by the silica cladding, which remains in place. Our SOI PhC structure also uses a substantially thicker core layer that is compatible with the smaller index contrast implied by retaining the silica lower cladding layer. The supported PhC channel guide configuration is inherently more robust and practically suitable. Our choice of device architecture is demonstrably an effective and flexible way of controlling the speed of light (down to the order of $c/99$) and its associated GVD, as described in Ref. 1.

We further carried out a detailed study of the effect of the input peak power level, and the impact of varying the slow-down factor on the nonlinear effects achievable in our proposed configuration for a photonic crystal channel waveguide, and have also shown the effect of the slow-down factor on the induced phase-shift at the optical frequency of the photonic bandgap. The transmitted spectrum becomes broader with increasing P_{in}, and develops multiple peaks when P_{in} is further increased due to the magnitude of the induced nonlinear refractive index, leading to a marked evolution of the optical frequency spectrum as the peak power level, P_{in}, is increased. The impact of the slow-down factor and the corresponding increase in nonlinear effects also defines the amount of input power required to achieve a particular level of spectral broadening in such waveguides. The present paper provides a comprehensive study of the effect of the slow-down factor and peak input power level on TPA, FCA, and the SPM produced in PhC channel waveguides. The large SPM response achieved in the structure is vital for applications such as optical switching, as shown in this paper. It has been reported[9] that femtosecond pulse propagation in SOI photonic wire waveguides can give rise to solitonic behavior. With appropriate rescaling, it becomes clear that the length of the PhC channel waveguide required to produce solitonic behavior will be greatly reduced by comparison with such fast photonic wire waveguides.

2 Slow Light Generation: Design Aspects

We have used an SOI-based photonic crystal structure with a hexagonal arrangement of *elliptical* air holes in a silicon core layer as the basis for analysis. The thickness of the underlying silica layer was chosen to be 3 μm, on top of which the silicon core layer was chosen to have

Downloaded From: http://nanophotonics.spiedigitallibrary.org/ on 09/07/2012 Terms of Use: http://spiedl.org/terms

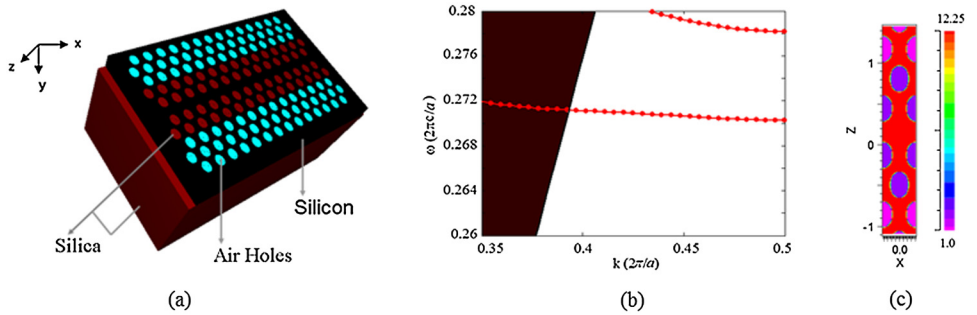

Fig. 1 (a) Schematic of the proposed structure with elliptical holes in a hexagonal arrangement. The two neighboring holes on either side of the waveguide are filled with silica rods. (b) The calculated dispersion curve for transverse electric polarization in the defect mode. The black solid line is the silica light line and the lower pointed red dispersion curve is used for calculating the group velocity. (c) Super-cell used in computation of the band structure.

a thickness equal to 0.443tpdel μm. The refractive index of silicon and silica are taken to be 3.49 and 1.45, respectively. A W0.7 waveguide was then created conceptually by omitting a row of air holes along the ΓK direction, and shifting the two photonic crystal regions closer to each other, so that the channel waveguide width becomes 0.7 times that of a W1 channel. The minimum values for the losses and defect mode dispersion below the silica light-line are found for a W0.7 waveguide. For this reason, one typical structure employed in experiments has been a W0.7 PhC waveguide.[18] The two neighboring rows of holes on either side of the waveguide are filled with silica rods. This partially in-filled configuration may require one or two additional stages in its fabrication, but the benefits of enabling better control of dispersion justify the modest increase in fabricational complexity that is implied.

The lattice constant a, semi-major radius r_1, and semi-minor radius r_2 of the elliptical air holes were 0.42, 0.16, and 0.118 μm, respectively. These parameters were obtained by properly optimizing the proposed structure to obtain a flat section of the dispersion curve below the silica light-line, because modes that lie above the light line are lossy in the vertical direction, i.e., into the substrate. Figure 1(a) shows a schematic of the proposed structure, and Fig. 1(b) shows the calculated dispersion curves for transverse electric (TE) polarized waves propagating in the defect mode. The flat section of the dispersion curve displays a slow group velocity over a substantial bandwidth. If we now define the low velocity range to be those values that give a $\pm 10\%$ variation in the group index n_g (Ref. 19), we obtain $n_g = 99$ over a frequency range of 344 GHz. Therefore, the normalized value of the delay-bandwidth product (DBP), which is defined as $n_g^*(\Delta\omega/\omega)$, is calculated to be 0.20.

We further investigated the delay for pulses propagating through the waveguide using finite-difference time-domain (FDTD) simulations. Figure 2 shows the field amplitude of the Gaussian

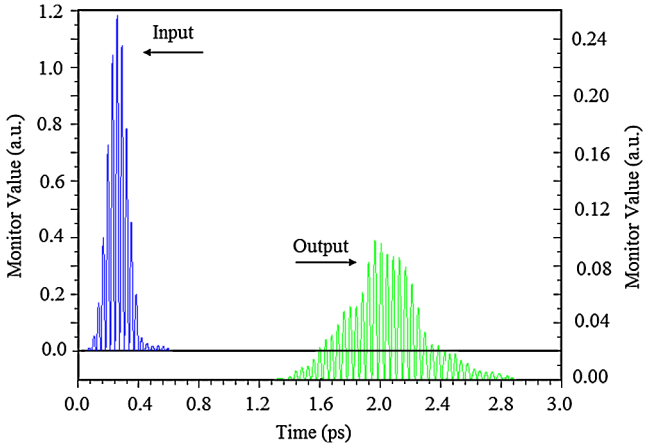

Fig. 2 Intensity of Gaussian pulse measured at the input and output ends of the waveguide, at $\lambda_0 = 1.55$ μm.

Downloaded From: http://nanophotonics.spiedigitallibrary.org/ on 09/07/2012 Terms of Use: http://spiedl.org/terms

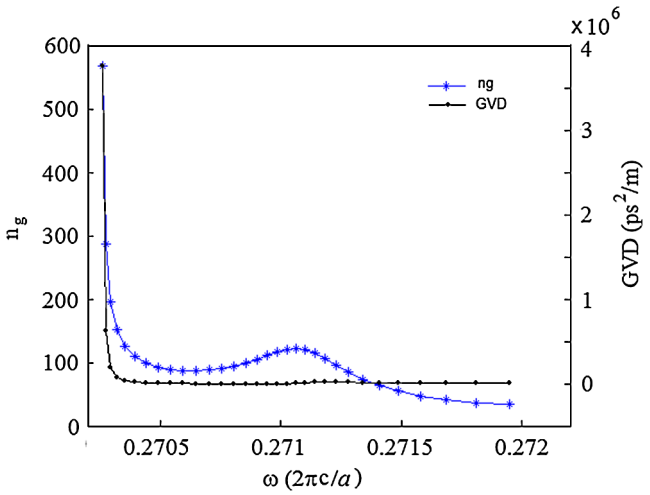

Fig. 3 Variation of group index and group velocity dispersion with frequency.

pulse recorded at the input and output ends of the waveguide, as a function of time, for $\lambda_0 = 1.55\ \mu$m. The length of the waveguide is $15a$. The GVD parameter β_2 is related to the second-order derivative of the dispersion curve by the following expression:

$$\beta_2 = \frac{d^2k}{d\omega^2} = \frac{d}{d\omega}\left(\frac{1}{d\omega/dk}\right) \Rightarrow \beta_2 = -\frac{1}{v_g^3}\frac{d^2\omega}{dk^2}. \tag{1}$$

The group velocity n_g and the GVD parameter, in the flat regime below the silica light line, are shown in Fig. 3 as a function of frequency. Figure 3 shows that the GVD parameter is on the order of 10^4 ps^2/m, and that the average group index is 99. We further define the slow-down factor S as the ratio of the group index n_g to the refractive index, n_{si}, of bulk silicon. It is calculated to be 28.28 at $\lambda_o = 1.55\ \mu$m for the designed elliptical hole PhC waveguide.

3 Nonlinear Modeling of Pulse Propagation

Next, we evaluated the nonlinearity of an SOI-based photonic crystal waveguide. The propagation of the optical pulse with amplitude $A(z,t)$ is given, for sufficiently strong confinement, by the following nonlinear Schrödinger equation[12,20,21] in one space dimension and time:

$$\frac{\partial A}{\partial z} + \frac{\alpha}{2}A + \left(\frac{i\beta_2}{2}\right)\left(\frac{\partial^2 A}{\partial t^2}\right) - \left(\frac{\beta_3}{6}\right)\left(\frac{\partial^3 A}{\partial t^3}\right) = i\kappa|A|^2A - N_c\left(\frac{\sigma}{2} + ik_c\,k_0\right)A, \tag{2}$$

where α accounts for the linear component of the propagation losses, β_2 is the dispersion parameter at wavelength λ_o, n_2 is the Kerr coefficient of silicon, κ defines the nonlinearity in the waveguide, given by: $\kappa = \gamma + i\zeta/2$, where $\gamma = 2\pi n_2/(\lambda_o A_{\text{eff}})$ is the nonlinear parameter, and ζ is related to the TPA coefficient, β_{TPA}, defined as $\zeta = \beta_{\text{TPA}}/2A_{\text{eff}}$. Here, A_{eff} is the cross-sectional area of the PhC channel waveguide mode and is found to be 0.12 μm^2 for slow modes ($S = 28.28$), whereas it is calculated to be 0.05 μm^2 ($S = 2$) for fast modes.[20] The second term on the right side of Eq. (2) gives the FCA, defined by the parameter σ, and FCD, accounted for by k_c, and N_c is the carrier density produced by TPA. In silicon, the free carriers generated by TPA are governed by the following rate equation:

$$\frac{\partial N_c(t)}{\partial t} = \frac{\beta_{\text{TPA}}}{2h\upsilon_o}|A|^4 - \frac{N_c}{\tau_c}, \tag{3}$$

where τ_c is the carrier lifetime of silicon and is taken to be approximately equal to 1 ns (Ref. 18). At $\lambda_o = 1.55\ \mu$m, the parameters identified in Eqs. (2) and (3) have the following values:[12,20] $n_2 = 6\times10^{-18}$ m^2/W, $\beta_{\text{TPA}} = 5\times10^{-12}$ m/W, $\sigma = 1.45\times10^{-21}$ m^2, $k_c = 1.35\times10^{-27}$ m^3,

Downloaded From: http://nanophotonics.spiedigitallibrary.org/ on 09/07/2012 Terms of Use: http://spiedl.org/terms

$\alpha = 20$ dB/cm $A_{\text{eff}} = 0.12\ \mu\text{m}^2$, the GVD and TOD are found to be $-8291\ \text{ps}^2/\text{m}$ and $-78\ \text{ps}^3/\text{m}$, respectively at $\lambda_o = 1.55\ \mu$m.

The reduction in the group velocity of the waveguide mode causes optical localization and field enhancement in the waveguide. The slow-down factor, S, may therefore be introduced into Eq. (2) by replacing α, γ, and β_{TPA}, by $\alpha \times S$, $\gamma \times S^2$, and $\beta_{\text{TPA}} \times S^2$, respectively. Equation (2) therefore becomes:

$$\frac{\partial A}{\partial z} + \frac{S\alpha}{2}A + \left(\frac{i\beta_2}{2}\right)\left(\frac{\partial^2 A}{\partial t^2}\right) - \left(\frac{\beta_3}{6}\right)\left(\frac{\partial^3 A}{\partial t^3}\right) = iS^2\gamma|A|^2A - \frac{S^2\beta_{\text{TPA}}}{2A_{\text{eff}}}|A|^2A - SN_c\left(\frac{\sigma}{2} + ik_c k_0\right)A. \tag{4}$$

When $T_0 \ll \tau_c$, and the pulse repetition rate is very low, the second term on the right side of Eq. (3), corresponding to carrier recombination, can be ignored because the recombination time, τ_c, is much larger than the pulse duration. Therefore, the carrier density profile of $N_c(t)$ near the input end of the waveguide for a Gaussian input pulse, with the temporal power profile is written as:

$$P(0,t) = P_{\text{in}}\ \exp(-t^2/T_0^2),$$

is found to be:

$$N_c(t) = \frac{S^2\beta_{\text{TPA}}P_{\text{in}}^2T_0}{2h\nu_o A_{\text{eff}}^2}\sqrt{\frac{\pi}{8}}\left[1 + \text{erf}\left(\frac{\sqrt{2}t}{T_0}\right)\right], \tag{5}$$

where P_{in} is the input peak power. For Gaussian pulses, the criterion for testing the relative magnitudes of FCA, FCD and TPA is given by the dimensionless parameter:[17] $r_a = (S\sigma P_{\text{in}}T_0\sqrt{\pi})/(2\sqrt{2}h\nu_o A_{\text{eff}})$. The scaling factor S is already included in this dimensionless parameter. For N_c to be negligible, $r_a \ll 1$ (i.e., the peak power should not be very high).

4 The Photonic Crystal Waveguide as a Soliton Propagator

According to standard soliton propagation theory,[15] a fundamental soliton can be excited if the condition $\gamma P_0 L_D = 1$ is satisfied, and also $\beta_2 < 0$. Furthermore, the time-domain expansion is simultaneously accompanied by spectral narrowing. This criterion was previously used as a test for soliton formation in silicon photonic waveguides.[9] The values obtained for the second and third-order dispersion coefficients at a wavelength of 1.55 μm are $\beta_2 = -8291\ \text{ps}^2/\text{m}$ and $\beta_3 = -78\ \text{ps}^3/\text{m}$. For Gaussian pulses, the criterion for testing the relative magnitudes of FCA, FCD, and TPA is given by the dimensionless parameter[17]: $r_a = (S\sigma P_{\text{in}}T_0\sqrt{\pi})/(2\sqrt{2}h\nu_o A_{\text{eff}})$. Here, N_c is negligible if $r_a \ll 1$ (i.e., the peak power should not be very high). If we now consider $P_{\text{in}} = 0.05$ W and $T_0 = 1$ ps, we obtain $r_a = 0.082 \ll 1$. For such low power levels, we can neglect the free-carrier density, N_c. Equation (4) can now be written as:

$$\frac{\partial A}{\partial z} + \frac{S\alpha}{2}A + \left(\frac{i\beta_2}{2}\right)\left(\frac{\partial^2 A}{\partial t^2}\right) - \left(\frac{\beta_3}{6}\right)\left(\frac{\partial^3 A}{\partial t^3}\right) = iS^2\gamma|A|^2A - \frac{S^2\beta_{\text{TPA}}}{2A_{\text{eff}}}|A|^2A. \tag{6}$$

For a waveguide of length $L = 150\ \mu$m, the above equation is solved using the split-step Fourier method. Here, $L_D = 120\ \mu$m and $L_{\text{NL}} = 123\ \mu$m, with $\gamma = 202\ \text{m}^{-1}\,\text{W}^{-1}$ and $P_{\text{in}} = 0.05$ W at $\lambda_0 = 1.55\ \mu$m.

The conditions for the propagation of a fundamental soliton are clearly satisfied. At low input power levels and low slow-down factors ($S = 1$), the impact of nonlinearity is negligible. Linear GVD broadens the pulse by a small amount in the time domain, but the pulse spectrum remains nearly unchanged. The pulse amplitude is reduced in magnitude because of linear losses [Figs. 4(c) and 4(d)]. However, for the same low peak power level in the input pulse, but a higher slow-down factor ($S = 28.28$), the temporal pulse broadening induced by linear dispersion is counteracted by the enhanced effect of TPA and the pulse width reduces considerably, in

Downloaded From: http://nanophotonics.spiedigitallibrary.org/ on 09/07/2012 Terms of Use: http://spiedl.org/terms

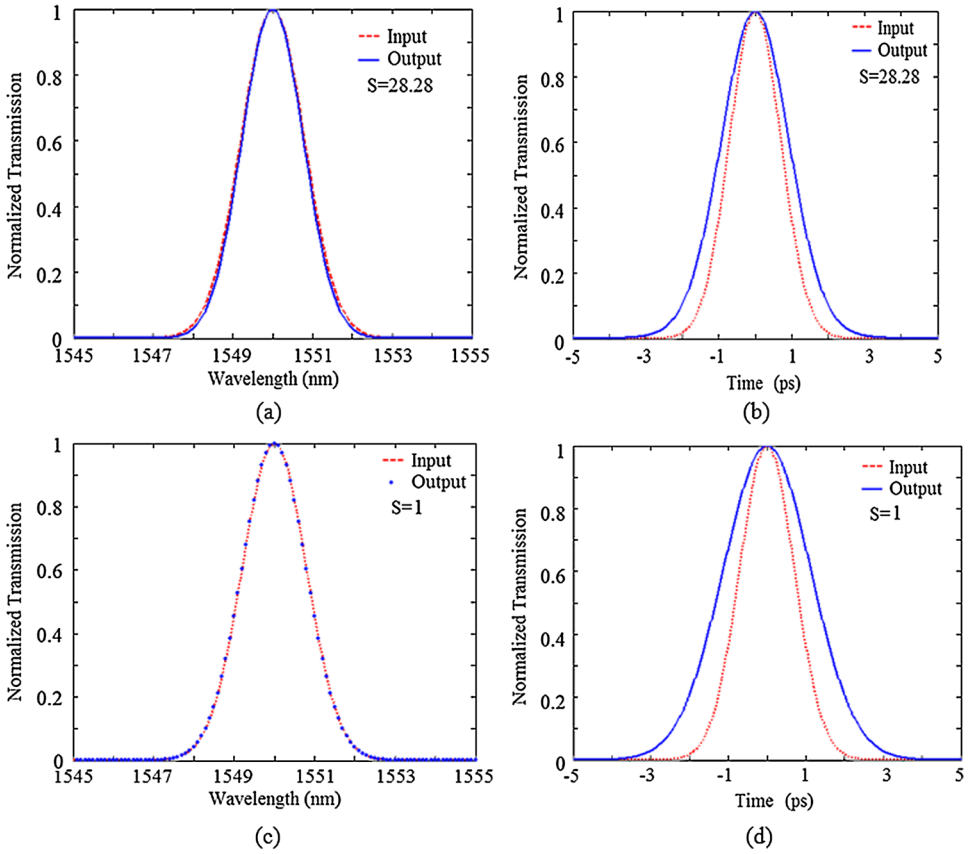

Fig. 4 Propagation of a 1 ps pulse through the SOI PhC waveguide; (a) and (c) spectrum, and (b) and (d) temporal pulse shapes for different slow-down factors, S.

comparison to faster waveguides ($S = 1$), as it propagates along the channel waveguide. The pulse adjusts its shape and evolves into a soliton-like pulse. Figures 4(a) and 4(b) show the input and output pulse profiles and corresponding spectra. For our choice of input pulse length, the output temporal spectrum contracts by a small amount (approximately 16%) with respect to that of the input pulse, and solitonic pulses are obtainable at peak input power levels as low as 50 mW.

5 Photonic Crystal Channel Waveguide as an Optical Spectral Switch

We now consider the effect of FCA and FCD, for the situation where the dimensionless parameter (Ref. 17), $r_a \gg 1$, for higher input power levels (0.5 W), and N_c is not negligible. As described in Sec. 1, the linear dispersion and nonlinearity in SOI-based PhC waveguides are characterized by their characteristic lengths, given by dispersion lengths L_D and $L_{D''}$, and the nonlinear length L_{NL}. For $T_0 = 1.4$ ps, at $\lambda_o = 1.55$ μm we have found:

$$L_D = \frac{T_0^2}{|\beta_2|} = 236\ \mu\mathrm{m}, \quad L_D'' = \frac{T_0^3}{|\beta_3|} = 3.5 \times 10^4\ \mu\mathrm{m}, \quad \text{and} \quad L_{\mathrm{NL}} = \frac{1}{S^2 \gamma P_{\mathrm{in}}} \approx 12.3\ \mu\mathrm{m}.$$

For a waveguide length of 150 μm, we have taken $S = 28.28$, $\gamma = 202\ \mathrm{m}^{-1}\mathrm{W}^{-1}$, and $P_{\mathrm{in}} = 0.5$ W. Because $L_{\mathrm{NL}} < L < L_D$, the dispersion effects in the waveguide have been ignored and the pulse evolution is therefore dominated by SPM and TPA, the latter of which is accompanied by free-carrier effects.[15] Hence, if we now neglect the GVD and TOD parameters from Eq. (4), it can be written as:

Downloaded From: http://nanophotonics.spiedigitallibrary.org/ on 09/07/2012 Terms of Use: http://spiedl.org/terms

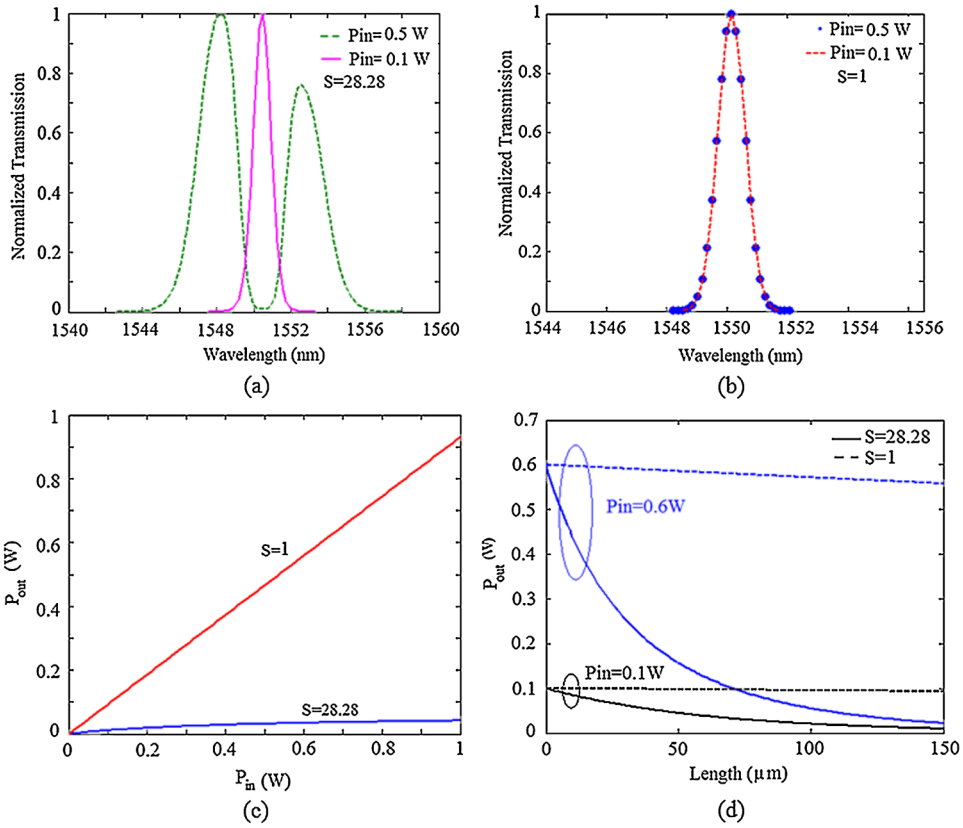

Fig. 5 Switching in the transmission spectrum of the SOI-based PhC channel waveguide at different input power levels and different slow-down factors; (a) $S = 28.28$, (b) $S = 1$. (c) Power-dependent transmission curves for different slow-down factors. (d) Variation of the output power along the length of the PhC waveguide.

$$\frac{\partial A}{\partial z} + \frac{S\alpha}{2}A = iS^2\gamma|A|^2A - \frac{S^2\beta_{\mathrm{TPA}}}{2A_{\mathrm{eff}}}|A|^2A - SN_c\left(\frac{\sigma}{2} + ik_ck_0\right)A. \tag{7}$$

Equation (7) is again solved using the split-step Fourier method and available values for the parameters of silicon. The input wavelength is chosen as 1.55 μm, which lies within the photonic bandgap. Figure 5(a) shows the signal that is transmitted through the waveguide when the peak incident power level is 0.1 W, which corresponds to the ON state at the output. When the incident peak power level is increased to 0.5 W, the transmission resonance at 1.55 μm is replaced by a transmission minimum. This low level output signal can be considered as the OFF state. This dramatic variation in the transmission spectrum is due to the changes in the refractive index induced by the nonlinear optical effects that include the Kerr effect and the FCD effect produced by TPA. Such effects we previously observed by Monat and colleagues in Ref. 16. However, when we compare the behavior of our structure with that of the structure considered in Ref. 16, it is found that similar switching behavior was obtained for $n_g = 40$ ($S = 11$), accompanied by a measured loss of approximately 27 dB (Ref. 16). Whereas, in our structure, the switching behavior was obtained for an input peak power level of only 0.5 W, and the overall losses at the output of the structure were well below 12 dB [Fig. 5(c)]. In our case, the possible significant contribution to the propagation losses that results from fabrication imperfections is not included in the model.

Figure 5 also displays the major role played by group velocity reduction in the nonlinear interaction. The Kerr effect is mainly responsible for the symmetric spectral broadening of the pulse. However, FCD also contributes to the spectral broadening, and is responsible for an additional overall blue-shift of the pulse spectrum. This blue-shift is due to the density of the free carriers generated by the pulse as it propagates through the medium, which results

Downloaded From: http://nanophotonics.spiedigitallibrary.org/ on 09/07/2012 Terms of Use: http://spiedl.org/terms

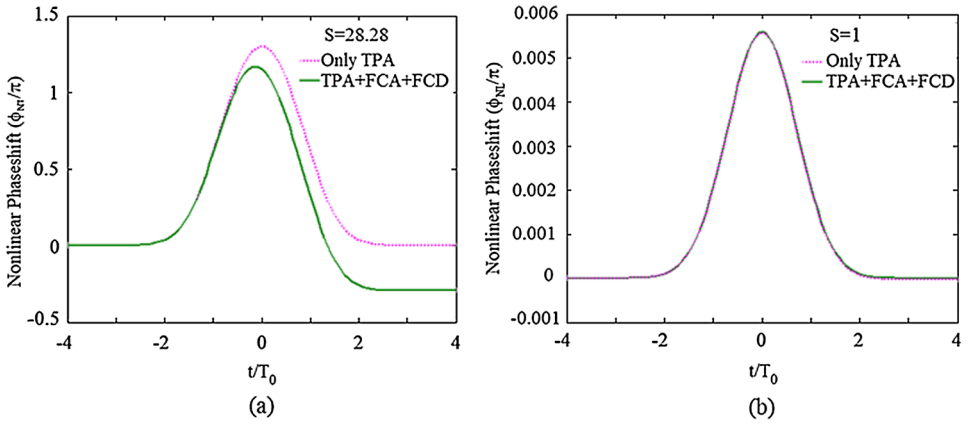

Fig. 6 Nonlinear phase shift showing the impact of TPA, FCA, and FCD for (a) $S = 28.28$ and (b) $S = 1$.

in a decrease in the refractive index of the silicon. This decrease creates an asymmetric and positive frequency chirp across the pulse, which causes the generation of a blue-shifted spectrum. A phase change of π induced in the proposed structure made from Si therefore switches the signal between its ON and OFF states over a restricted range of wavelengths that is approximately centered on 1.55 μm, and hence the photonic crystal channel waveguide acts as a form of all-optical switch. However, for fast waveguides, with $S = 1$, the impact of the Kerr effect and FCD is not appreciable, and this wavelength-dependent switching action is not seen in such waveguides [Fig. 5(b)]. These results show that the amount of phase change was strongly affected by the slow-down factor S, and hence by the nonlinear parameters, such as the TPA parameter, ζ, and the Kerr nonlinear parameter, γ, which scale with the square of the slow-down factor, and the FCA parameter, σ, and the FCD parameter, k_c, which scale directly with the slow-down factor, S. Figure 5(d) shows the calculated optical power distribution along the waveguide. The presence of TPA in slower waveguides, with $S = 28.28$, causes strong attenuation of the light, and loss of most of the input power near the input end of the waveguide, because of the strong dependence of the nonlinear behavior on the velocity of light inside the waveguide. However, in faster waveguides with $S = 1$, the light is attenuated by only a small amount after propagation through a 150-μm-long PhC waveguide.

These results are consistent with those obtained experimentally by Baron et al. in GaAs PhC channel waveguides.[22] However, because it is primarily the Kerr effect that is sought for the nonlinear optical manipulation, TPA may be regarded as a hindrance. With the values of the Kerr coefficient, n_2, being equal to 1.6×10^{-17} m^2/W in GaAs and 0.5×10^{-17} m^2/W in Si, but the TPA coefficient for GaAs being much larger, as compared with silicon, in the relevant wavelength range, larger values for the Kerr phase-shift are obtainable in Si than in GaAs. In contrast, the larger total magnitude of the nonlinearity in GaAs has been successfully exploited to modify the resonant behavior of high Q-factor PhC microcavities.[23]

The nonlinear phase shift, ϕ_{NL}, introduced into the incident wave by the TPA, FCA, and FCD effects, is shown in Figs. 6(a) and 6(b). It was observed that the phase profile is symmetric for the case where only TPA is significant. However, it becomes asymmetric and attains negative values when both FCA and FCD are included. The blue-shift observed is due to the negative values observed in the nonlinear phase-shift. Figures 6(a) and 6(b) show that the phase-shift due to these nonlinear parameters is enhanced linearly for slower waveguides ($S = 28.28$) in comparison with faster waveguides ($S = 1$). Note the very different vertical scales in Figs. 6(a) and 6(b).

6 The Spectral Broadening Factor

We now introduce the spectral broadening factor, f. The spectral broadening factor for a Gaussian pulse is given by:[15,17]

Downloaded From: http://nanophotonics.spiedigitallibrary.org/ on 09/07/2012 Terms of Use: http://spiedl.org/terms

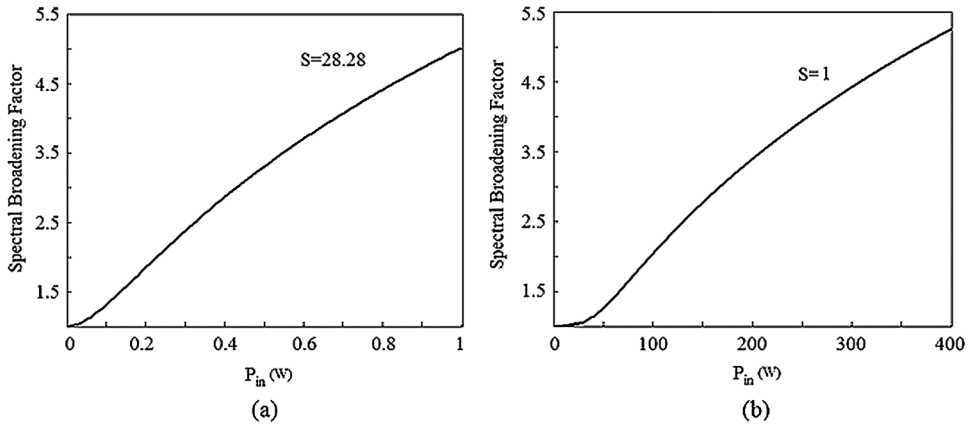

Fig. 7 Variation of spectral broadening factor f with input power density for, (a) $S = 28.28$ and (b) $S = 1$.

$$f = \left(1 + \frac{4}{3\sqrt{3}}\phi_{\mathrm{NL}}^2\right)^{1/2}, \tag{8}$$

where $\phi_{\mathrm{NL}}(L, 0)$ is the nonlinear phase-shift induced in the PhC waveguide due to the effects of TPA, FCA, and FCD. The results in Figs. 7(a) and 7(b) show the spectral broadening as a function of the input power density level, at two different slow-down factor values, $S = 28.28$ and $S = 1$, respectively.

For a particular slow-down factor, at high input power levels, TPA limits the maximum spectral broadening and is responsible for the saturation behavior. It was also demonstrated that spectral broadening is greater in slow waveguides than in fast waveguides. A much higher input power level is required to obtain the same level of spectral broadening in fast waveguides as in slow waveguides. Note the very different horizontal scales in Figs. 7(a) and 7(b).

7 Discussion and Comparisons

It is appropriate, before concluding this paper, to reexamine our results in comparison with others who have already appeared in the literature, e.g., the work described in Refs. 14, 16, 20, and 22. Firstly, comparison with the work of Baron et al. [22] indicates that TPA is arguably a more important effect in slow-light PhC waveguides fabricated in GaAs than for structures fabricated in silicon, because the TPA coefficient for GaAs in the relevant wavelength range is substantially larger than that of silicon. The larger TPA coefficient implies that the nonlinear behavior of slow-light devices realized in GaAs is, at the wavelengths with which we are concerned, dominated by the much larger refractive index change produced by TPA in GaAs than in silicon, as well as the larger absorption in GaAs.

Ikeda and Fainman,[24] in an important paper that deserves to be more widely read and understood, show that the nonlinear, Kerr-effect based, figure-of-merit (FOM) of materials relevant to this study, at wavelengths close to 1.55 μm, is substantially larger for silicon than for GaAs, but is still small. The FOM takes account both of the n_2 coefficient of the material (which is three times larger for GaAs than for silicon) and the attenuation, which because of the much greater [by more than 10 times (Ref. 24)] TPA coefficient of GaAs, is much greater in GaAs than in silicon. The end result is that the FOM for GaAs is about three times *smaller* than that of silicon. A further comparison, and one that is vitally important for practical all-optical devices, should also be made when the waveguide in which the slow-light PhC structure is realized in the epitaxially grown ternary compound $Al_xGa_{1-x}As$, with progressively greater x-fraction. The greater the value of x, the greater is the direct electronic bandgap of the material, whereas the n_2 coefficient progressively declines. At $x = 18\%$, the nonlinear FOM is already one order of magnitude greater in $Al_xGa_{1-x}As$ than in silicon, whereas at $x = 36\%$, the FOM has increased by a further order of magnitude. The slow-light structure of Inoue et al.[14] was based on $Al_xGa_{1-x}As$ material

Downloaded From: http://nanophotonics.spiedigitallibrary.org/ on 09/07/2012 Terms of Use: http://spiedl.org/terms

with $x = 26\%$, and indicates a FOM that is approximately 40 times greater than that of silicon.

In this paper, we show that, at comparable power density levels and slowing factor values, silicon based PhC slow-light waveguides can be realized as effectively in relatively thick silicon waveguide cores supported by a silica cladding,[1] with no cover material, as in unsupported (and therefore inherently fragile) thin silicon membranes. Furthermore, we show that the dispersion control, which is required for soliton formation and broadband delay enhancement, can be obtained simply by moving from a PhC structure based on circular holes (with several different hole diameters being required in a single structure) to a specific choice of elliptical hole parameters in uniform arrays of elliptical holes. Our estimate of the in-waveguide optical power required to obtain a decisive wavelength-selective switching effect is 0.5 W, at a group velocity of $c/99$, whereas Monat and colleagues[16] require a peak power level of 45 W at a group velocity of $c/50$. This apparently large superiority for our structure, in practice, will be substantially eroded for slow-light propagation in structures with the propagation losses due to scattering that have been experimentally achieved to date.

Confidence in our formulation of the nonlinear propagation problem in slow-light PhC waveguides realized in silicon comes from recognition that it is essentially identical to that used in the work of Refs. 16, 20, and 22. Furthermore, the broad similarity of the results shown [for example, in Fig. 5(a) of this paper, Fig. 3 of Ref. 14, Figs. 2 and 3 of Ref. 20, Figs. 4 and 6 of Ref. 16, and Fig. 3 of Ref. 23] indicates a consistent situation for both simulation and experiment. The TPA dominated result of Fig. 3 in Ref. 23 is notable because it only requires 0.5 W peak power, together with a group velocity that has been reduced only to $c/9$. Therefore, where TPA is an acceptable process for slow-light enhanced propagation modification, GaAs scores significantly by comparison with silicon. But the acceptability of using TPA becomes much reduced if the pulse repetition rate increases to values above 1 GHz and/or the photo-excited carrier lifetime is sufficiently long, e.g., substantially greater than 1 ns. The almost purely Kerr nature of the nonlinear behavior of sufficiently large bandgap ternary alloy $Al_xGa_{1-x}As$ suggests that devices realized in this material merit further investigation at substantially reduced group velocities, i.e., in the region of $c/50$.

8 Conclusion

In this paper, we reported the design of an SOI-based PhC channel waveguide with elliptical holes. Two neighboring rows on either side of the channel waveguide are filled with silica rods to obtain an average group index of 99 at a wavelength of 1550 nm. We further carried out the nonlinear modeling of the wave propagation in such a waveguide, and a detailed study of the effect of input peak power and different slow-down factors on the nonlinear effects achieved in proposed photonic crystal channel waveguide was presented. If the input pulse width is in the hundred-femtosecond regime, the waveguide can generate soliton-like propagation at moderate pulse energies of 50 mW. This type of slow-light structure has considerable potential for use in photonic device applications, such as optical switches at an input peak power level of 500 mW. The impact of FCA and the index changes induced by FCD on the amplitude and phase of optical pulses was also studied in this paper. The spectral broadening factor calculated for the waveguide shows that a higher input power level (on the order of 10^2 W) is required to obtain the same level of spectral broadening in fast waveguides as in slow waveguides at a power level of approximately 1 W.

Acknowledgments

The authors gratefully acknowledge the initiatives and support towards establishment of the "TIFAC Centre of Relevance and Excellence in Fiber Optics and Optical Communication at the Delhi College of Engineering, Delhi" through the "Mission REACH" program of Technology Vision-2020 of the Government of India. Two of the authors (R.K. Sinha and Richard M. De La Rue) are also grateful to the Royal Academy of Engineering (UK) for providing financial support to carry out collaborative research and development work in the area of Photonic Crystal Devices.

Downloaded From: http://nanophotonics.spiedigitallibrary.org/ on 09/07/2012 Terms of Use: http://spiedl.org/terms

References

1. S. Rawal, R. K. Sinha, and R. M. De La Rue, "Slow light miniature devices with ultra-flattened dispersion in silicon-on-insulator photonic crystal," *Opt. Exp.* **17**(16), 13315–13325 (2009), http://dx.doi.org/10.1364/OE.17.013315.
2. T. F. Krauss, "Slow light in photonic crystal waveguides," *J. Phys. D: Appl. Phys.* **40**(9), 2666–2670 (2007), http://dx.doi.org/10.1088/0022-3727/40/9/S07.
3. M. Soljacic and J. D. Joannopoulos, "Enhancement of nonlinear effects using photonic crystals," *Nat. Mater.* **3**, 211–219 (2004), http://dx.doi.org/10.1038/nmat1097.
4. M. D. Settle et al., "Flat band slow light in photonic crystals featuring spatial pulse compression and terahertz bandwidth," *Opt. Exp.* **15**(1), 219–226 (2007), http://dx.doi.org/10.1364/OE.15.000219.
5. L. H. Frandsen et al., "Photonic crystal waveguides with semi slow light and tailored dispersion properties," *Opt. Exp.* **14**(20), 9444–9450 (2006), http://dx.doi.org/10.1364/OE.14.009444.
6. H. Oda et al., "Light amplification by stimulated Raman scattering in AlGaAs based photonic crystal line defect waveguides," *Appl. Phys. Lett.* **93**(5), 051114 (2008), http://dx.doi.org/10.1063/1.2965110.
7. V. N. Astratov et al., "Heavy photon dispersions in photonic crystal waveguides," *Appl. Phys. Lett.* **77**(2), 178–180 (2000), http://dx.doi.org/10.1063/1.126916.
8. H. Tsang et al., "Optical dispersion, two photon absorption and self phase modulation in silicon waveguides at 1.5 μm wavelength," *Appl. Phys. Lett.* **80**(3), 416–418 (2002), http://dx.doi.org/10.1063/1.1435801.
9. W. Ding et al., "Solitons and spectral broadening in long silicon-on-insulator photonic wires," *Opt. Exp.* **16**(5), 3310–3319 (2008), http://dx.doi.org/10.1364/OE.16.003310.
10. P. Millar et al., "Nonlinear propagation effects in an AlGaAs Bragg grating filter," *Opt. Lett.* **24**(10), 685–687 (1999), http://dx.doi.org/10.1364/OL.24.000685.
11. X. Chen Nicolae et al., "Third order dispersion and ultrafast pulse propagation in silicon wire waveguides," *IEEE Phot. Tech. Lett.* **18**(24), 2617–2619 (2006), http://dx.doi.org/10.1109/LPT.2006.887214.
12. L. Yin and G. P. Agrawal, "Impact of two photon absorption on self phase modulation in silicon waveguides," *Opt. Lett.* **32**(14), 2031–2033 (2007), http://dx.doi.org/10.1364/OL.32.002031.
13. H. Oda et al., "Self phase modulation in photonic crystal slab line defect waveguides," *Appl. Phys. Lett.* **90**(23), 231102 (2007), http://dx.doi.org/10.1063/1.2746068.
14. K. Inoue et al., "Enhanced third order nonlinear effects in slow light photonic crystal slab waveguides of line defect," *Opt. Exp.* **17**(9), 7206–7216 (2009), http://dx.doi.org/10.1364/OE.17.007206.
15. G. P. Agrawal, *Nonlinear Fiber Optics III*, Academic Press, San Diego (2001).
16. C. Monat et al., "Slow light enhanced nonlinear optics in silicon photonic crystal waveguides," *IEEE J. Select. Top. Quant. Elect.* **16**(1), 344–357 (2010), http://dx.doi.org/10.1109/JSTQE.2009.2033019.
17. Q. Lin, O. J. Painter, and G. P. Agrawal, "Nonlinear optical phenomena in silicon waveguides: Modeling and applications," *Opt. Exp.* **15**(25), 16604–16644 (2007), http://dx.doi.org/10.1364/OE.15.016604.
18. M. Notomi et al., "Single mode transmission within photonic bandgap of width varied single line defect photonic crystal waveguide on SOI substrates," *Electron. Lett.* **37**(5), 293–295 (2001), http://dx.doi.org/10.1049/el:20010195.
19. Y. Hamachi, S. Kubo, and T. Baba, "Slow light with low dispersion and nonlinear enhancement in a lattice shifted photonic crystal waveguide," *Opt. Lett.* **34**(7), 1072–1074 (2009), http://dx.doi.org/10.1364/OL.34.001072.
20. C. Monat et al., "Slow light enhancement of nonlinear effects in silicon engineered photonic crystal waveguides," *Opt. Exp.* **17**(4), 2944–2953 (2009), http://dx.doi.org/10.1364/OE.17.002944.
21. I. D. Rukhlenko et al., "Nonlinear pulse evolution in silicon waveguides: an approximate analytic approach," *IEEE J. Lightwave Technol.* **27**(15), 3241–3248 (2009).

Downloaded From: http://nanophotonics.spiedigitallibrary.org/ on 09/07/2012 Terms of Use: http://spiedl.org/terms

22. A. Baron et al., "Light localization induced enhancement of third order nonlinearities in a GaAs photonic crystal waveguide," *Opt. Exp.* **17**(2), 552–557 (2009), http://dx.doi.org/10.1364/OE.17.000552.
23. S. Combrié et al., "GaAs photonic crystal cavity with ultrahigh Q: microwatt nonlinearity at 1.55 μm," *Opt. Lett.* **33**(16), 1908–1910 (2008), http://dx.doi.org/10.1364/OL.33.001908.
24. K. Ikeda and Y. Fainman, "Material and structural criteria for ultra-fast Kerr nonlinear switching in optical resonant cavities," *Solid State Electron.* **51**(10), 1376–1380 (2007), http://dx.doi.org/10.1016/j.sse.2007.06.012.

Swati Rawal has been awarded the PhD degree in 2011 from Delhi College of Engineering, Faculty of Technology, University of Delhi, India. Her current research interests include photonic crystal waveguides, devices and slow light in photonic crystals. She is recipient of ''SPIE Best Research Paper Award" for her research paper related to slow light in photonic crystals during the Internal Conference on Optics and Photonics-2009 held at CSIO Chandigarh, India. She is also recipient of student leadership award from Optical Society of America for participating in the international conference ''Frontiers in Optics" held in San Jose, CA, USA during October 10 to 15, 2009. She has worked as senior scientific officer at TIFAC-CORE, Mission REACH program of Technology Vision-2020, Delhi Technological University, Delhi, from February to December 2011. Currently, she is working as assistant professor in Physics Department, S. G. T. B. Khalsa College, University of Delhi.

Ravindra K. Sinha received his MSc degree in physics from the Indian Institute of Technology (IIT), Kharagpur, India, in 1984, and his PhD degree in fiber optics and optical communication from the IIT, Delhi, India, in 1990. Later he worked on various research and academic positions during 1990 and 1998. He is currently professor and head of Applied Physics Department, and the chief coordinator of the TIFAC–CORE in Fiber Optics and Optical Communication at Delhi Technological University (formerly DCE), Delhi. He is the author or co-author of more than 180 research publications in the leading national and international journals and conference proceedings and chapters in books. He was awarded Emerging Optoelectronics Technology Award [(CEOT-IETE, India)]-2006 for outstanding research work in the area of nanophotonics, S. K. Mitra Memorial Award for in Best Research Paper in IETE Technical Review 2002. He is a fellow of the IETE (India), Faculty Adviser of SPIE-DCE Chapter and OSA-DCE Chapter at Delhi Technological University.

Richard De La Rue was appointed as lecturer at Glasgow University in 1971, became a senior lecturer in 1982, a reader in 1985, and professor of optoelectronics in 1986. His research is particularly concerned with photonic crystal and photonic wire structures, waveguide microcavities and metamaterials. His research in the area of photonic crystals has evolved to cover compact lasers, planar microcavities, photonic-crystal LEDs, synthetic opal and inverse opal structures. His historic interest in lithium niobate integrated optics is currently reviving in the context of photonic crystal structure fabrication. He has published more than 200 articles and papers in journals and as book chapters. He is a fellow of the IEEE (FIEEE, 2003); fellow of the OSA (OSA Fellow 2007)—and fellow of the Royal Academy of Engineering (FREng, 2002), fellow of the Royal Society of Edinburgh (FRSE, 1989) and fellow of the Institution of Engineering and Technology (FIET/FIEE, 1997).

Downloaded From: http://nanophotonics.spiedigitallibrary.org/ on 09/07/2012 Terms of Use: http://spiedl.org/terms